Energy loss of low-energy electrons to nonabrupt metal surfaces

F. Forstmann,* A. Gras-Marti,† T. L. Ferrell, R. J. Warmack, and K. C. Mamola
Health and Safety Research Division, Oak Ridge National Laboratory, Oak Ridge, Tennessee 37831-6123
(Received 6 July 1990; revised manuscript received 10 April 1991)

The interaction of a charged particle with a semi-infinite medium bounded by a flat surface is analyzed as a problem of metal optics. The reflection at the surface of the electromagnetic fields excited by the passing beam is investigated including retardation and spatial dispersion in the hydrodynamic approximation. The soft decay of the electron density at the metal-vacuum interface is modeled. Using measured values of the dielectric function, the calculations are found to agree with experimental results of electron-energy-loss distributions for Ag targets in interaction at a distance. Further predictions of the theoretical model are discussed.

I. INTRODUCTION

The analysis of the interaction of energetic electrons with polarizable materials provides interesting information about the collective response of the electronic system in the exposed media. Constant improvements in the experimental techniques, both at high electron energies[1] ($\sim$100 keV) and at low energies[2] ($\sim$1 keV), often raise questions that existing theory is unable to answer completely. Even in the conceptually simpler experiments where only aloof electron trajectories are monitored, and little interference from bulk effects is expected on the measurable electron energy losses, the variety of target geometries investigated experimentally[3] (planar targets, cubes, spheres, cylinders, etc.) pose difficult problems for the theoretical modeling.[4] The situation is further complicated by the fact that a complete description of the electromagnetic response of the medium is not always available for those geometries. It is in this context that we believe that a different theoretical approach to the analysis of beam-surface interactions may be valuable.

The calculation of the energy-loss spectrum and the stopping power for charged particles that are moving near conducting surfaces is treated here as a problem in metal optics. This approach is different from other treatments in the literature on aloof beam-surface interactions. The stopping power will be related to the reflection coefficient at the surface, appropriate for plane waves emanating from the moving charge. The reflection coefficient is calculated in the hydrodynamic approximation, which is capable of including in a straightforward manner the excitation of charge-density perturbations near the surface, the damping of plasma waves, the excitation of band transitions via a measured dielectric function, and the retardation of the field propagation due to the finite velocity of light. A similar calculation was recently published for the jellium model.[5] There exist several publications that study the response of the electron gas at a jellium surface.[6] These calculations demonstrate that, in jellium, the mechanism for energy absorption near the surface is caused by breaking of translational symmetry at the surface. But it has been shown[6–9] that the frequency dependence of the absorption probability is determined mainly by the behavior of the electromagnetic field derived via the bulk dielectric function including the collective excitations, and not by matrix-element effects or by the surface-induced Friedel oscillations. These results justify the use of the hydrodynamic approximation, which treats these fields correctly, in an attempt to study the response of Ag surfaces, which cannot be treated as jellium. With this approach we are able to use the measured bulk dielectric function $\epsilon(\omega)$ as a basis for the surface response.

In a previous paper[10] some of us have reported energy-loss measurements of low-energy (30–1200 eV) electrons which have passed through microchannels of $\approx$20–200 nm in diameter in thin Ag foils. The dominant structure in the loss-probability curve was a peak around the surface plasmon energy at 3.6 eV. As the present calculations will show, the energy-loss probability per unit path length traveled by the electron decays so strongly with increasing distance from the surface that the losses occur at distances to the surface which are small compared to the diameter of the channels. Therefore, the curvature of the channel walls is considered unimportant for the understanding of the measurements. In Ref. 10, the analysis of the experiments was carried out under the following main approximations: (a) the electrons are coupled instantaneously to the charges induced on the metal (neglect of retardation), (b) the induced charge is a singular surface charge, and (c) the bulk of the metal is free of induced charge. Assumptions (b) and (c) are implied by the neglect of spatial dispersion, whereby one describes the response of the metal by a dielectric function which is independent of the wave vector of the exciting field. It has been shown[5] that retardation effects are important for the electron energy of interest in the experiments mentioned above.[10]

In this paper, we lift approximations (a), (b), and (c). In essence, we find that the dispersion of the surface plasmons shifts the main energy loss peak, which represents a weighted average over the surface-plasmon density of states, to higher energies, actually higher than the measurements show. In order to explain the mea-

surements, the soft decay of the metal charge density at the surface has to be taken into consideration. This effect is caused by the well-known finite screening length of the electron gas.[11] The smoothness of this density drop can be extended by microscopic roughness, which, by averaging laterally, can be modeled as a metal layer of lower electron density. Our calculations show that such a model shifts the energy-loss peak to lower frequencies. This conclusion also helps in understanding the fact that the peak position found experimentally was dependent on the condition of preparation of the perforated Ag films. The effect of roughness on the measured electron-energy-loss spectra has been discussed recently.[2]

In the following section, we derive the energy-loss probability per unit path length for an electron flying parallel and external (aloof) to a metal surface, including spatial dispersion in the hydrodynamic approximation, and also including retardation in the calculation. In Sec. III, we compare the theoretical results with the experimental data, and some model predictions are presented. Some conclusions follow in Sec. IV.

II. ENERGY LOSS OF A TRAVELING CHARGE

Take a particle of charge q traveling outside a semi-infinite dielectric medium and parallel to its surface, Fig. 1. If x is the direction of motion, the stopping power of the particle, or energy loss per unit path length traveled, is

$$-\frac{dW}{dx}=qE_x \tag{1}$$

with W the energy of the particle, and E_x the x component of the reaction electric field at the location of the particle. This part of the total electric field is due to the charges induced in the metal by the bypassing charge q and is calculated under the assumption that the particle velocity is constant during the interaction. Ordinary calculations of the stopping power in aloof electron-solid interaction are based on the semiclassical dielectric approach.[5,12–14] In this paper, the calculation of E_x will be considered as a problem of metal optics. The charge moving above the metal surface is a source of fields according to Maxwell's equations. These electromagnetic waves impinge on the metal surface with which they interact and, after reflection, form the induced field at the location of the charged particle. Due to the negative x component of the induced field, the particle is slowed down, Fig. 1.

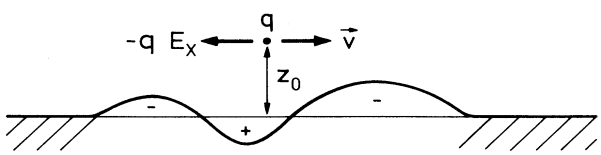

FIG. 1. The induced charge density near the moving electron.

The metal occupies the half-space $z<0$. If $\mathbf{r}=(x,y,z)$ is the position vector of the charge and $\mathbf{R}=(x,y,0)$ is its x-y projection, a charge with density

$$\rho(\mathbf{r},t)=q\delta(\mathbf{R}-\mathbf{v}t)\delta(z-z_0)$$

moves in vacuum with velocity $\mathbf{v}=(v,0,0)$ and at a distance z_0 from the metal surface (see Fig. 1). The moving charge carries with it a field in vacuum which is given by

$$\mathbf{E}_0(\mathbf{K},z,\omega)=-\frac{q}{2\pi\lambda}\left[\frac{\omega}{c^2}\mathbf{v}-\mathbf{k}\right]\times\exp(i\lambda'|z-z_0|)\delta(\omega-\mathbf{K}\cdot\mathbf{v}) \tag{2}$$

with c the velocity of light, $\mathbf{k}=(k_x,k_y,\pm\lambda')$ a wave vector, ($k_z=\lambda'$ for $z>z_0$, $k_z=-\lambda'$ for $z<z_0$), $\mathbf{K}=(k_x,k_y,0)$, and

$$\lambda'=+\left[\frac{\omega^2}{c^2}-K^2\right]^{1/2}. \tag{3}$$

In Eq. (2) we operate with the two-dimensional Fourier transforms of the fields, which are defined by

$$\mathbf{E}_0(\mathbf{r},t)=\int d\mathbf{K}\int d\omega\, e^{i(\mathbf{K}\cdot\mathbf{R}-\omega t)}\mathbf{E}_0(\mathbf{K},z,\omega)\,. \tag{4}$$

Equation (4) represents the particle field as a superposition of plane waves incident on the metal surface. We decompose these plane waves in linearly polarized waves, which are parallel or perpendicular to the plane of incidence, p or s waves, respectively. The s-polarized component is perpendicular to both $\mathbf{k}$ and $\mathbf{u}_z$ (the normal to the target surface),

$$\mathbf{E}_{0s}=(\mathbf{E}_0\cdot\mathbf{u}_s)\mathbf{u}_s \tag{5a}$$

with

$$\mathbf{u}_s=\frac{\mathbf{k}\times\mathbf{u}_z}{|\mathbf{k}\times\mathbf{u}_z|}=\left[\frac{k_y}{K},-\frac{k_x}{K},0\right], \tag{5b}$$

and the p-polarized component is parallel to a plane containing the z axis and the vector $\mathbf{K}$,

$$\mathbf{E}_{0p}=\mathbf{E}_0-\mathbf{E}_{0s}=\frac{(\mathbf{E}_0\cdot\mathbf{K})}{K^2}\mathbf{K}+\mathbf{E}_{oz}\,. \tag{5c}$$

Each component of the field is reflected by the surface. In terms of the reflection coefficient r_s, the amplitude of the s-polarized component of the reflected field at the surface is

$$\mathbf{A}_s=r_s\mathbf{E}_{0s}\quad(z=0)\,. \tag{6}$$

The z component of the electric field of the p-polarized wave is reflected with an amplitude

$$A_{pz}=r_pE_{0z}\quad(z=0)\,, \tag{7}$$

in terms of the reflection coefficient r_p, while the amplitude of the component which is tangential to the surface is determined by[15]

$$\mathbf{A}_{p,tg}=-\frac{\lambda'}{K^2}A_{pz}\mathbf{K} \ . \tag{8}$$

With r_s and r_p given, the x component of the induced field sums up to

$$A_x=A_{sx}+A_{px}=\frac{k_y}{K^2}r_s(E_{0x}k_y-E_{0y}k_x)-\frac{\lambda' k_x}{K^2}r_pE_{0z} \ . \tag{9}$$

Exploiting the fact that $\mathbf{E}_0$ is divergence-free outside the metal, we eliminate E_{0y} from Eq. (9),

$$A_x=-\frac{\lambda' k_x}{K^2}(r_s+r_p)E_{0z}+r_sE_{0x} \ . \tag{9'}$$

The x component of the total induced field is

$$E_x(\mathbf{r},t)=\int d\mathbf{K}\int d\omega\, e^{i(\mathbf{K}\cdot\mathbf{R}+\lambda' z-\omega t)}A_x(\mathbf{K},\omega) \ . \tag{10}$$

Equations (1)–(3), (9), and (10) combined yield the stopping power

$$-\frac{dW}{dx}=\frac{q^2}{2\pi v^2}\int dk_y\int\omega\, d\omega\, e^{2i\lambda' z_0}\left[\frac{\lambda'}{K^2}(r_s+r_p)+\frac{1}{\lambda'}\left[1-\frac{v^2}{c^2}\right]r_s\right]_{k_x=\omega/v} \tag{11}$$

with the integrand evaluated at $k_x=\omega/v$. From the requirement that the real incoming field is reflected into a real outgoing field, it follows that

$$r_{s,p}(-\mathbf{K},-\omega)=r^*_{s,p}(\mathbf{K},\omega) \ .$$

We take $\lambda'=-i\lambda$, or

$$\lambda=\left[K^2-\frac{\omega^2}{c^2}\right]^{1/2} , \tag{12}$$

which is a real quantity for $k_x=\omega/v$, and realize that r_p and r_s, for fixed k_x and ω, must not depend on the sign of k_y. These arguments together allow us to finally write

$$-\frac{dW}{dx}=\frac{2q^2}{\pi v^2}\int_0^\infty\int_0^\infty dk_y\, d\omega\,\omega\, e^{-2\lambda z_0}\mathrm{Im}\left[-\frac{\lambda}{K^2}(r_s+r_p)+\frac{1}{\lambda}\left[1-\frac{v^2}{c^2}\right]r_s\right]_{k_x=\omega/v} \tag{13}$$

with the integrand still evaluated at $k_x=\omega/v$. The Fourier coefficient in the frequency expansion of $-dW/dx$ is interpreted as the probability of losing energy in the interval $(\hbar\omega, d(\hbar\omega))$, per unit traveled path length,

$$-\frac{dW}{dx}=\int_0^\infty\hbar\omega\frac{d^2P}{dx\, d(\hbar\omega)}d(\hbar\omega) \ . \tag{14}$$

The excitation probability per unit path length is the quantity that we shall compare with experimental data.

The problem of the interaction between the traveling charge and the metal surface has been reduced to the calculation of the reflection amplitudes for the plane waves emanating from the charge. If we neglect spatial dispersion, we can immediately make use of Fresnel formulas, which, in our notation, read[15]

$$\begin{aligned} r_s&=\frac{\lambda-k}{\lambda+k} \ , \\ r_p&=\frac{\epsilon\lambda-k}{\epsilon\lambda+k} \ , \end{aligned} \tag{15}$$

with λ defined in Eq. (12), $\epsilon=\epsilon(\omega)$, and

$$k=\left[K^2-\epsilon\frac{\omega^2}{c^2}\right]^{1/2} . \tag{16}$$

Now, if retardation is neglected ($c\to\infty$), it follows that

$$\lambda=k=K=(k_y^2+\omega^2/v^2)^{1/2} \ ,$$

and

$$-\frac{dW}{dx}=\frac{2q^2}{\pi v^2}\int_0^\infty d\omega\,\omega\,\mathrm{Im}\left[-\frac{\epsilon-1}{\epsilon+1}\right]K_0\left[\frac{2\omega z_0}{v}\right] , \tag{17}$$

a result that was first reported by Echenique and Pendry.[18] This is the expression used in Ref. 10 in the comparisons with experimental data. K_0 is a zeroth-order Bessel function.[16]

In this work we include spatial dispersion in the response of the metal, and also retardation effects. In the calculation of the reflection coefficients we include spatial dispersion, in the so-called hydrodynamic approximation. The hydrodynamic approximation, whereby the frequency and wave-vector-dependent dielectric function $\epsilon(\omega,\mathbf{k})$ is approximated up to terms in k^2, includes the excitation of charge-density perturbations in the metal, the damping of plasma waves, the excitation of band transitions via measured $\epsilon(\omega)$, and the retardation of the field propagation. Maxwell's equations have, within this approximation, the (longitudinal) plasma waves as additional homogeneous solutions to the general solutions inside the metal. At an interface between homogeneous media, the general solutions in each medium are matched by additional boundary conditions. The capabilities of the hydrodynamic approximation can be seen from a comparison of the fields near the surface with those derived from microscopic calculations.[8,9]

In the hydrodynamic approximation, the k dependence is introduced into the longitudinal dielectric function according to an approximation which has been used successfully for other optical investigations.[17,18] The measured complex dielectric function $\epsilon(\omega)$ is separated into a part due to free electrons and a part due to bound electrons. Only the (longitudinal) free-electron system is assumed to show spatial dispersion,

$$\epsilon_1(\omega,\mathbf{k})=\epsilon_b(\omega)-\frac{\omega_n^2}{\omega^2-\beta k^2}\ . \tag{18}$$

The parameter ω_n, the plasma frequency of an equivalent electron gas, is usually determined from a fit of $\epsilon(\omega)$ to infrared data, with the assumption $\epsilon_b(\omega)=1$ at those frequencies. For Ag, $\hbar\omega_n=9$ eV, which corresponds to one electron per Ag atom. The parameter β has been measured[19] for Ag to amount to $\beta=2.57\times10^{12}\ \mathrm{m}^2/\mathrm{s}^2$.

In order to model the soft decrease of the charge density at the surface due to the finite screening length of the electron gas and due to surface roughness, we assume (see Fig. 2) a surface layer of thickness d ($\simeq$3–6 Å) with smaller free-electron density n_s, i.e., with parameters $\omega_s^2=\omega_n^2 n_s/n_0$ and $\beta_s=\beta(n_s/n_0)^{2/3}$. n_0 is the bulk electron density. This two-step surface model also allows us to investigate the response of metal layers deposited on a substrate.[9] At the interface of the homogeneous regions, boundary conditions are needed to match the homogeneous solutions.[9,20]

After having specified our surface model for the spatially dispersive metal, it requires the solution of a system of seven linear equations to find the amplitude of the reflected wave in the case of p polarization in the two-step model. The derivation of r_p and r_s is described in detail in Ref. 9 and the resulting expressions will be given in the Appendix for the vacuum-metal case and for the two-step model of the electron density near the surface. If one takes the limit of an abrupt surface, and neglects spatial dispersion and retardation ($d\to0$, $\mu\to\infty$, and $c\to\infty$) in the expressions obtained with this more general approach (see the Appendix), one retrieves the expression in Eq. (17) for the stopping power. The electrostatic result in Eq. (17) will be used as a reference in our discussion.

III. ANALYSIS AND COMPARISON WITH EXPERIMENTAL RESULTS

We shall investigate the dependence of the excitation probability $d^2P/[dx\,d(\hbar\omega)]$ defined by Eqs. (13) and (14) on the distance from the surface, the energy of the particle, and the parameters of the metallic surface layer. We shall also compare the different approximations which have been derived for r_s and r_p, and the influence of retardation on the energy-loss process.

We compare in Fig. 3, for the case of a sharp interface ($d=0$), for two electron energies and for $z_0=10$ Å, the

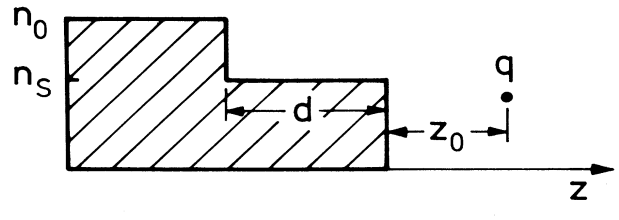

FIG. 2. Our surface model. The charge q moves at a distance z_0 from a surface layer of density n_s located on top of the bulk of the metal of density n_0.

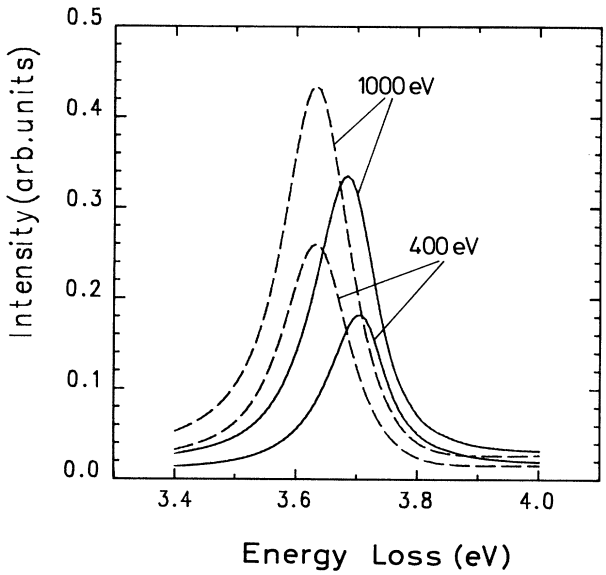

FIG. 3. The energy-loss intensity calculated with (——) and without (— — —) spatial dispersion for two energies of the incoming electron. For a sharp-step surface and $z_0=10$ Å.

excitation probability predicted by the model which includes spatial dispersion in the response of the medium, with the limit evaluated in Eq. (17). It is found that the effect of spatial dispersion is to shift the energy-loss peak to higher energies. The surface plasmon frequency $\omega_s(k)$ is given by the zero of N_{den} in Eq. (A4) in the Appendix, but this dispersion is neglected in the calculation that leads to the result in Eq. (17). Without spatial dispersion being accounted for, all surface plasmons lie at the frequency ω_{s0} given by the zero of the denominator in the loss function in Eq. (17), i.e., by $\epsilon(\omega_{s0})=-1$, while the inclusion of the k dependence in the dielectric response leads to the (linear) increase of ω_s above ω_{s0}, with growing k. The shift of the loss peak becomes smaller with increasing velocity of the charged particle because the relation $k_x=\omega/v$ carries the weight for surface plasmon excitation toward smaller values of k_x; that is, toward frequencies which are closer to ω_{s0}. The position of the resonance peak does not change with the distance from the electron to the surface as we shall see below.

The measured peak is at a lower energy than the peaks calculated for a surface with a sharp electron-density step. In order to bring the calculated peak position to the measured peak, it has been argued that the density gradient of electrons near the surface and surface roughness lower the resonance energy. In Ref. 2 the roughness has been modeled by spheres the size of which was adjusted and averaged. The model used here simulates the soft decrease of the free-electron density leaking out of the positive background.[11] The model consists of a layer of reduced density on top of the bulk density (Fig. 2), therefore approximating the density gradient by two steps. This model was successful previously.[9,20] The parameters of the selvedge (d in Å and n_s/n_0, see Fig. 2) can be interpreted as also accounting for some averaging over roughness.

Figure 4 shows the dependence of the loss spectrum on the parameters of the soft-surface model. The shift in the peak position depends essentially on the decrease in total charge in the surface layer, $\Delta\sigma=d(n_0-n_s)$. The peak of the loss distribution is shifted toward lower energies whenever the width of the surface step increases for a given reduced surface density, or when the density is decreased for a given layer thickness.

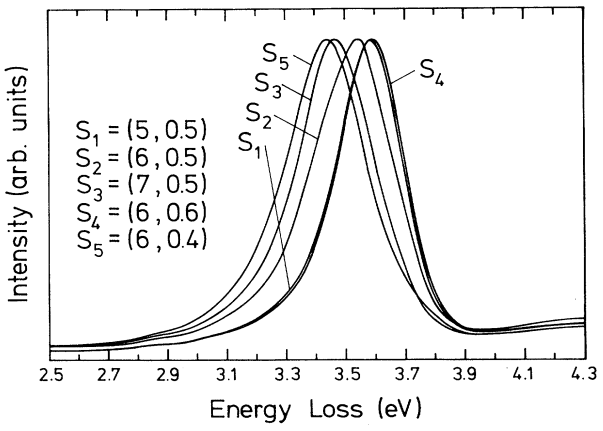

FIG. 4. The dependence of the loss spectrum on the model parameters of the surface density step. All curves normalized to the peak value. The electron energy is 900 eV, and $z_0=10$ Å. The step parameters are d in Å and n_s/n_0.

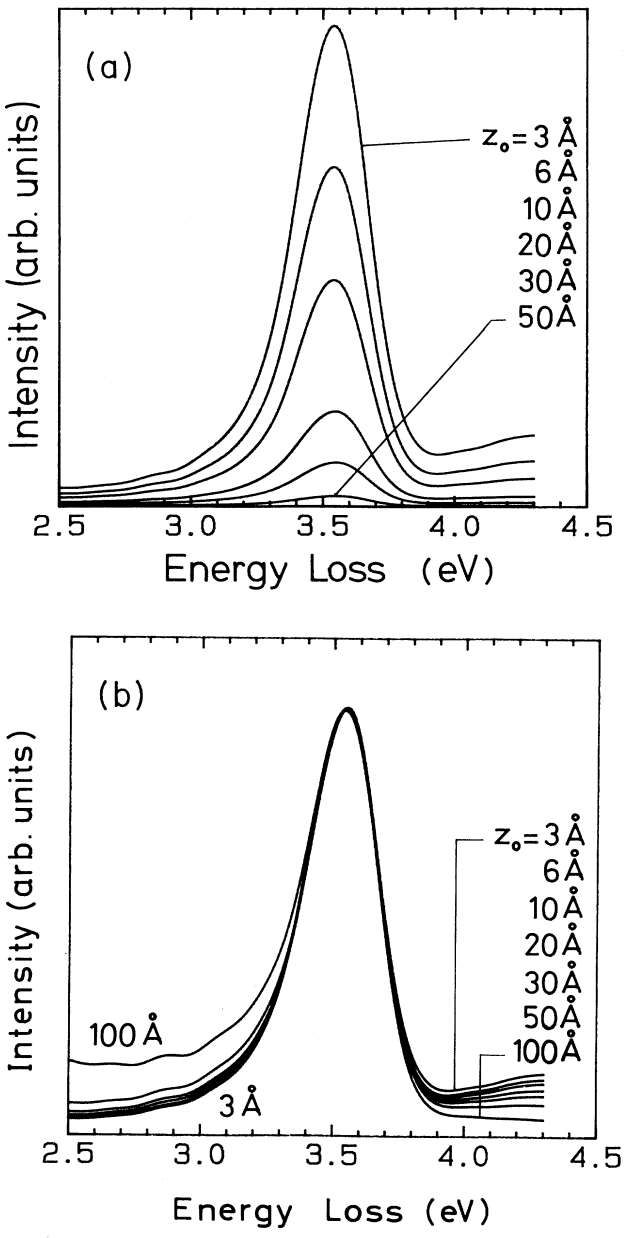

FIG. 5. Dependence of the loss spectrum on electron distance from the surface. (a) Decrease of loss intensity. (b) The same shape for all distances. Step parameters: 6 and 0.5, $E_{\text{kin}}=900$ eV.

For reasonable values of the parameters d and n_s/n_0, the best fit of the calculated peak position with the experimental data of Ref. 2 is obtained for a surface step 6 Å wide, with half the bulk density (6|0.5). This set of parameters is to be adopted in the following calculations. Furthermore, all theoretical curves, except those in Fig. 3, are broadened with the experimental resolution of Refs. 2 and 10.

Next we study the dependence of the loss distribution on the distance z_0 from the particle to the surface. We choose our optimized step $d=6$ Å and $n_5/n_0=0.5$ and an electron energy of 900 eV (Fig. 5). The loss intensity is strongly decaying with increasing distance [Fig. 5(a)], but when the curves are normalized to the same peak value they all have the same shape in the distance range of relevance, Fig. 5(b). We exploit this fact by neglecting the averaging over distances when comparing our predictions with the experimental results of Refs. 2 and 10.

The influence of the electron kinetic energy E_{kin} on the excitation probability is shown in Fig. 6(a). For increasing E_{kin}, the position of the peak, Fig. 6(b), first moves to smaller energy losses $\hbar\omega$, then goes through a minimum, and finally increases again, but even for $E_{\text{kin}}=10$ keV the peak still lies far from the position predicted by the abrupt-surface electrostatic model, Eq. (17). The minimum in peak position is directly related to a minimum in the surface-plasmon dispersion because, as mentioned earlier, the high velocity particles excite the small-k_x plasmons. The minimum in surface plasmon dispersion is due to the decay of the electron density at the surface.[9] Looking at the experimental results in Fig. 4 of Ref. 10, one can notice the shift of the loss maximum toward higher loss energies for increasing particle velocity.

We compare in Fig. 7 the predictions of the soft-surface model developed in this paper with the experimental data from Refs. 2 and 10. The agreement between theory and experiment is very good. In the calculation presented in Ref. 2 the electrons lost energy to metallic spheres and the peak position was adjusted by choosing spheres 13 nm in diameter. These spheres should approx-

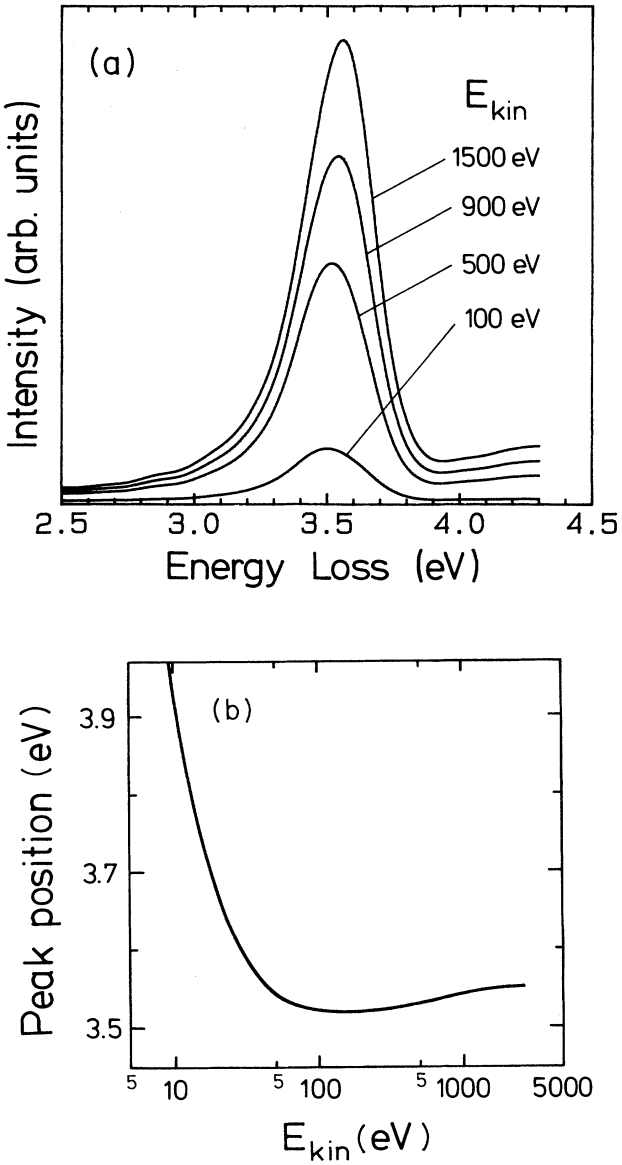

FIG. 6. (a) Dependence of the loss spectrum on electron kinetic energy. (b) The peak position vs kinetic energy of the electron.

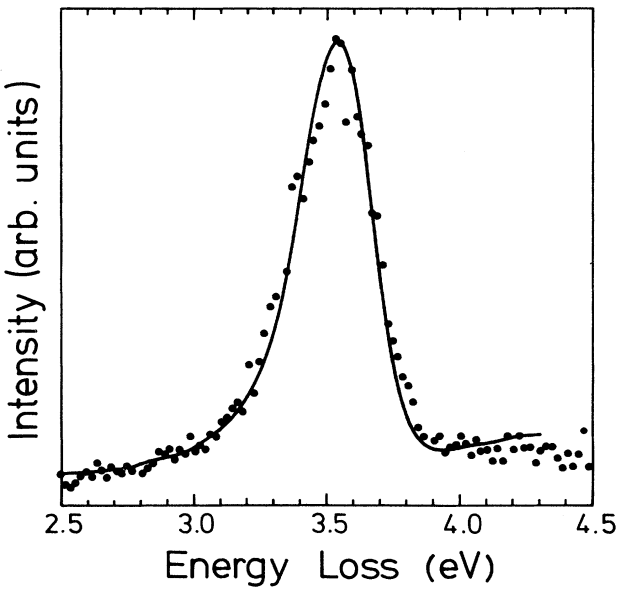

FIG. 7. Comparison of the loss spectrum calculated for the surface model 6 and 0.5 with the experimental results of Refs. 2 and 10.

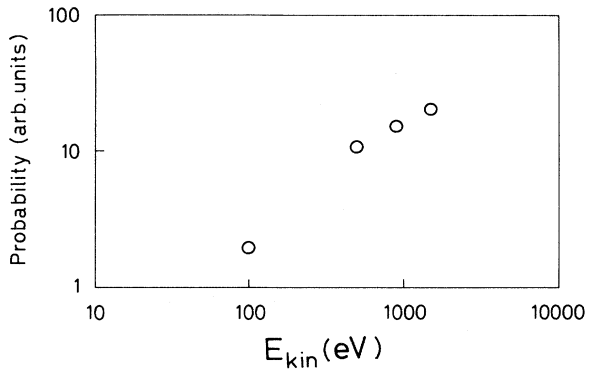

FIG. 8. Dependence of the integrated loss spectrum on the kinetic energy of the electron. Step parameters 6 and 0.5.

imate protruding roughness. Our model is equivalent to averaging over roughness of size smaller than the plasmon wavelength. Furthermore, our model takes into account the dispersion of the surface plasmon.

We have seen in Fig. 6(a) that the probability of excitation of the resonance mode increases with electron energy. The experimental work of Ref. 10 included a presentation of integrated probability with respect to impact energy. In order to compare that result with the predictions of our model, we have applied a similar procedure, as described in Ref. 10, to treat our theoretical results: the differential excitation probability in Fig. 6(a) has been integrated over the range of 2.5–4 eV, subtracting a straight-line background formed by connecting those two points. The results, shown in Fig. 8, reproduce the behavior seen in Fig. 5 of Ref. 10. The integrated excitation probability increases by an order of magnitude when the electron energy changes from 100 to 1500 eV. Since there are some uncertainties[21] in the procedure used for background subtraction in Ref. 10, a more quantitative comparison is not attempted here.

IV. CONCLUSIONS

We have analyzed previous measurements of the energy-loss probability of electrons passing through narrow channels in a Ag foil by a calculation which takes into account the spatial dispersion of the response function of the metal. The calculation is done in the hydrodynamic approximation. The corresponding dispersion of the surface plasmon results in a shift of the loss peak toward higher energies compared to the results predicted by standard optics.

The fact that the measured loss peak lies even lower than the nonlocal calculation predicts can be understood by taking into account the decrease of the free-electron density at the surface. This decrease is due to the electrons leaking out of the positive background, as well as due to the existence of roughness on the surface on a microscopic scale. A fit of the model parameters to the experimental points gives a measure of the roughness. It should be interesting to check this prediction by comparing to measurements done on foils prepared at lower evaporation temperatures, where one expects rougher surfaces.

In conjunction with further experimental studies, one hopes that the previous discussion of the effect of the variations of the model parameters on the excitation probability will contribute toward clarifying the respective ranges of applicability of the present theory and the model developed in Ref. 2. Further calculations based on the present model, for different materials and including calculation of the image force, are in progress.

ACKNOWLEDGMENTS

This research was supported in part by the Spanish DGICyT (Project Nos. PS88-0066 and PS89-0065), and in part by the Office of Health and Environmental Research and the U.S. Department of Energy under Contract No. DE-AC05-84OR21400 with Martin Marietta Energy Systems, Inc. Two of us (F.F. and A.G.-M.) would like to express their gratitude for the hospitality of the Biological and Radiation Physics Section (HASRD) at Oak Ridge National Laboratory. A.G.-M. acknowledges the hospitality of the Freie Universität during the completion of this project.

APPENDIX: EXPRESSIONS FOR r_s AND r_p IN THE HYDRODYNAMIC APPROXIMATION (REF. 9)

1. One interface: Vacuum-metal

$$r_p=\frac{\lambda\epsilon-k+(K^2/\eta)[(\epsilon-\epsilon_b)/\epsilon_b]}{\lambda\epsilon+k-(K^2/\eta)[(\epsilon-\epsilon_b)/\epsilon_b]}\ , \tag{A1}$$

where now $\epsilon=\epsilon_b-\omega_n^2/\omega^2$, λ is given by Eq. (12), k by Eq. (16), and

$$\eta=\left[K^2-\frac{\omega^2\epsilon}{\beta^2\epsilon_b}\right]^{1/2}\ . \tag{A2}$$

The result for r_s is not modified from the one given in Eq. (15).

2. Two interfaces: Vacuum–surface layer–bulk metal

The results for a two-step surface model of a metal are given here. As shown in Fig. 2, we take a layer (thickness d) of lower electron density (n_s) on top of a semi-infinite bulk metal (density n_0). The reflection amplitude for s polarization is not affected by spatial dispersion. It has the simple form

$$r_s=\frac{(\lambda+k)(\theta-k)e^{-2kd}-(\lambda-k)(\theta+k)}{(\lambda-k)(\theta-k)e^{-2kd}-(\lambda+k)(\theta+k)} \tag{A3}$$

with $k=[K^2-(\omega^2/c^2)\epsilon_1]^{1/2}$, in the surface layer, and

$$\theta=[K^2-(\omega^2/c^2)\epsilon_2]^{1/2}$$

in the bulk. The resulting expression for p polarization is more cumbersome

$$r_p = N_{\text{num}}/N_{\text{den}} \tag{A4}$$

with

$$N_{\text{num}} = C_{MM}F_1 + C_{PM}F_2 e^{-2kd} + C_{MP}F_3 e^{-2\eta d} + C_{PP}F_4 e^{-2(k+\eta)d} - F_5 e^{-(k+\eta)d} ,$$

$$N_{\text{den}} = C_{PP}F_1 + C_{MP}F_2 e^{-2kd} + C_{PM}F_3 e^{-2\eta d} + C_{MM}F_4 e^{-2(k+\eta)d} + F_5 e^{-(k+\eta)d} ,$$

$$F_1 = \left[1+\frac{\eta}{\mu}\right] + \frac{\epsilon_b}{\epsilon_2}\frac{\epsilon_2-\epsilon_1}{\epsilon_1-\epsilon_b}\frac{B_{PP}}{B_P} ,$$

$$F_2 = \left[1+\frac{\eta}{\mu}\right]\frac{B_M}{B_P} + \frac{\epsilon_b}{\epsilon_2}\frac{\epsilon_2-\epsilon_1}{\epsilon_1-\epsilon_b}\frac{B_{MM}}{B_P} ,$$

$$F_3 = F_1 - 2\frac{\eta}{\mu} ,$$

$$F_4 = F_2 - 2\frac{\eta}{\mu}\frac{B_M}{B_P} , \quad F_5 = 8kK^2\frac{\epsilon_2-\epsilon_b}{\mu B_P} ,$$

$$C_{PP(MM)} = \lambda\epsilon_1 + (-)k + (-)\frac{K^2}{\eta}\frac{\epsilon_1-\epsilon_b}{\epsilon_b} ,$$

$$B_{PP(MM)} = k\epsilon_2 + (-)\theta\epsilon_1 + (-)\frac{K^2}{\mu}(\epsilon_2-\epsilon_1) ,$$

$$B_{P(M)} = k\epsilon_2 + (-)\theta\epsilon_1 ,$$

$$\epsilon_1(\omega) = \epsilon_b(\omega) - \frac{\omega_n^2 n_s/n_0}{\omega^2} ,$$

$$\epsilon_2(\omega) = \epsilon_b(\omega) - \frac{\omega_n^2}{\omega^2} = \epsilon_{\text{measured}} ,$$

$$\eta = \left[K^2 - \frac{\omega^2}{\beta_s}\frac{\epsilon_1}{\epsilon_b}\right]^{1/2} , \quad \mu = \left[K^2\frac{\omega^2}{\beta}\frac{\epsilon_2}{\epsilon_b}\right]^{1/2} .$$

Note also that, as indicated after Eq. (11), $K^2 = \omega^2/v^2 + K_y^2$. The parameters β and β_s are defined after Eq. (18). (As a mnemonic help, in the expressions above P stands for plus sign and M for minus sign.)

---

*Permanent address: Institut für Theoretische Physik, Freie Universität, Arnimallee 14, D-1000 Berlin 33, Germany.

†Permanent address: Departament de Física Aplicada, Universitat d'Alacant, Apt. 99, E-03080 Alacant, Spain.

[1]A. Howie, in Report of the Tenth Werner Brandt Workshop on Penetration Phenomena, Alacant, Spain, 1987 (ORNL Report No. CONF-870155.

[2]K. C. Mamola, R. J. Warmack, and T. L Ferrell, Phys. Rev. B **35**, 2682 (1987).

[3]L. D. Marks, Solid State Commun. **43**, 727 (1982); A. Howie and R. H. Milne, Ultramicroscopy **16**, 279 (1985); J. M. Cowley, Prog. Surf. Sci. **21**, 209 (1986).

[4]L. Dobrzynski and A. A. Maradudin, Phys. Rev. B **6**, 3810 (1972); A. Moussiaux, A. Ronveaux, and A. Lucas, Can. J. Phys. **55**, 1423 (1977); A. D. Boardman, R. Garcia-Molina, A. Gras-Martí, and E. Louis, Phys. Rev. B **32**, 6045 (1985); R. Garcia-Molina, A. Gras-Martí, and R. H. Ritchie, *ibid.* **31**, 121 (1985).

[5]Tran Thoai Duy Bao, Phys. Status Solidi B **139**, 145 (1987).

[6]For reviews see, P. J. Feibelmann, Prog. Surf. Sci. **12**, 287 (1982); A. Liebsch, Phys. Scr. **35**, 354 (1987).

[7]B. N. J. Persson and E. Zaremba, Phys. Rev. B **31**, 1863 (1985).

[8]K. Kempa and F. Forstmann, Surf. Sci. **129**, 516 (1983).

[9]F. Forstmann and R. R. Gerhardts, *Metal Optics Near the Plasma Frequency,* Vol. 109 of *Springer Tracts in Modern Physics* (Springer-Verlag, Berlin, 1986), p. 1.

[10]R. J. Warmack, R. S. Becker, V. E. Anderson, R. H. Ritchie, Y. T. Chu, J. Little, and T. L. Ferrell, Phys. Rev. B **29**, 4375 (1984).

[11]N. D. Lang and W. Kohn, Phys. Rev. B **1**, 4555 (1970).

[12]P. M. Echenique, Ph.D. thesis, University of Cambridge, 1976; P. M. Echenique and J. B. Pendry, J. Phys. C **8**, 2936 (1975).

[13]A. Howie, Ultramicroscopy **11**, 141 (1983).

[14]R. Garcia-Molina, A. Gras-Martí, A Howie, and R. H. Ritchie, J. Phys. C. **18**, 5335 (1985).

[15]L. D. Landau and E. M. Lifshitz, *Electrodynamics of Continuous Media* (Pergamon, New York, 1960), p. 273.

[16]M. Abramowitz and I. A. Stegun, *Handbook of Mathematical Functions* (Dover, New York, 1972).

[17]F. Forstmann, Z. Phys. B **32**, 385 (1979); F. Forstmann, K. Kempa, and D. M. Kolb, J. Electroanal. Chem. **150**, 241 (1983).

[18]F. Abelés and T. López-Rios, in *Surface Polaritons,* edited by V. M. Agranovich and D. L. Mills (North-Holland, Amsterdam, 1982), Chap. 6.

[19]G. Piazza, D. M. Kolb, K. Kempa, and F. Forstmann, Solid State Commun. **51**, 905 (1984).

[20]F. Forstmann and H. Stenschke, Phys. Rev. Lett. **38**, 1365 (1977).

[21]R. J. Warmack (private communication).